

# UC Berkeley

## UC Berkeley Previously Published Works

### Title

Tethered ligands reveal glutamate receptor desensitization depends on subunit occupancy

### Permalink

<https://escholarship.org/uc/item/4bx575pf>

### Journal

Nature Chemical Biology, 10(4)

### ISSN

1552-4450

### Authors

Reiner, Andreas

Isacoff, Ehud Y

### Publication Date

2014-04-01

### DOI

10.1038/nchembio.1458

Peer reviewed



# HHS Public Access

Author manuscript

*Nat Chem Biol.* Author manuscript; available in PMC 2014 October 01.

Published in final edited form as:

*Nat Chem Biol.* 2014 April ; 10(4): 273–280. doi:10.1038/nchembio.1458.

## Tethered ligands reveal glutamate receptor desensitization depends on subunit occupancy

Andreas Reiner<sup>1</sup> and Ehud Y. Isacoff<sup>1,2,\*</sup>

<sup>1</sup>Department of Molecular and Cell Biology and Helen Wills Neuroscience Institute, University of California Berkeley, Berkeley, California 94720

<sup>2</sup>Physical Bioscience Division, Lawrence Berkeley National Laboratory, Berkeley, California 94720

### Abstract

Cell signaling is often mediated by the binding of multiple ligands to a multi-subunit receptor. The probabilistic nature and slow rate of binding of diffusible ligands at low concentrations can impede attempts to determine how ligand occupancy controls signaling in such protein complexes. We describe a solution to this problem that uses a photoswitched tethered ligand as a “ligand clamp” to induce rapid and stable binding and unbinding at defined subsets of subunits. We applied the approach to study gating in ionotropic glutamate receptors (iGluRs), ligand-gated ion channels that mediate excitatory neurotransmission and plasticity at glutamatergic synapses in the brain. We probed gating in two kainate-type iGluRs, GluK2 homotetramers and GluK2/GluK5 heterotetramers. Ultrafast (sub-millisecond) photoswitching of an azobenzene-based ligand on specific subunits provided a real-time measure of gating and revealed that partially occupied receptors can activate without desensitizing. The findings have implications for signaling by locally released and spillover glutamate.

### Introduction

Much of membrane signaling is mediated by ligand binding to specific receptors. Typically these are multimeric protein complexes with multiple binding sites, which allows for steep and fine-tuned dose-response properties, the integration of diverse signals, and functional versatility. However, the contribution of individual binding sites on the functional state of a receptor and their cooperative interactions are often difficult to assess, because the association and dissociation of diffusible ligands is stochastic.

We demonstrate a generalizable solution to this problem that employs a covalently tethered photoswitchable ligand as a “ligand clamp”, analogously to how the voltage clamp works

Users may view, print, copy, download and text and data- mine the content in such documents, for the purposes of academic research, subject always to the full Conditions of use: [http://www.nature.com/authors/editorial\\_policies/license.html#terms](http://www.nature.com/authors/editorial_policies/license.html#terms)

\*Correspondence to: ehud@berkeley.edu, 510-642-9853.

Author contributions

A.R. and E.Y.I. designed experiments, A.R. performed and analyzed experiments, and A.R. and E.Y.I. wrote the manuscript.

Competing financial interests

The authors declare no competing financial interests.

for voltage-gated channels. The key to the voltage clamp is its ability to step voltage from one stable level to another more quickly than the response rate of the channels so that gating can be followed in real-time. The closest approximation for ligand-gated channels has been rapid piezo-driven solution exchange, but even at high ligand concentrations this method cannot resolve ligand-induced gating in the fastest proteins and at sub-saturating ligand concentrations the rate of equilibration becomes considerably slower. Even after binding reaches steady state, ligands constantly bind and unbind, which results in varied occupancies across molecularly identical proteins and confounds analysis. We show how a tethered ligand controlled by an azobenzene photoswitch solves these problems by virtually clamping the ligand to the binding site of specific subunits.

We applied the approach to ionotropic glutamate receptors (iGluRs), an important family of ligand-gated ion channels at excitatory synapses in the central nervous system. The three main classes of iGluRs<sup>1-4</sup>, AMPA, kainate and NMDA receptors, transmit excitatory signals across the synaptic cleft and control synaptic strength and plasticity, processes key to learning and memory formation. All iGluRs assemble from four subunits, and many are functional as homotetramers. However, *in vivo* they are typically heteromers of different subunit types and isoforms<sup>2</sup>, which diversifies their functional properties, as receptors combine high and low affinity subunits or incorporate subunits with distinct protein interaction domains for downstream effectors.

AMPA and kainate receptors operate on very fast timescales. Receptor activation, including glutamate binding and channel opening, occurs in less than a millisecond<sup>1,2</sup>. In the presence of sustained ligand binding, desensitization, a temporary inactivation of the receptors, terminates the current flow within a few milliseconds. The desensitization and recovery kinetics sculpt the postsynaptic current, set the response to subsequent glutamate release events and limit the ion flow in potentially pathophysiological situations<sup>3</sup>. Desensitization is highly regulated and controlled by subunit composition, alternative splicing<sup>5</sup> and accessory subunits<sup>6</sup>. Its physiological importance is also highlighted by mutations causing profound developmental phenotypes<sup>7</sup> and pharmaceutical agents modulating this process<sup>2</sup>.

The overall architecture of iGluRs was revealed by functional and structural studies<sup>2,8,9</sup>. The four ligand binding domains (LBDs) are organized as a pair of dimers. Ligands bind in the central cleft of the bilobed, clam shell-like domains and high efficacy agonists seem to close the LBDs more effectively than low efficacy agonists or antagonists<sup>10,11</sup>, which apparently provides more driving force for pore opening. Desensitization has been accounted for by structural rearrangements at the LBD dimer interface, and mutations, cross-linkers, and allosteric modulators stabilizing the interface can slow or abolish desensitization<sup>2,12-20</sup>.

A key aspect to the gating mechanism of iGluRs is how the occupancy of the four ligand binding sites in the two LBD dimers drives receptor activation and desensitization<sup>8,21,22</sup>. A seminal single molecule experiment established that binding of two agonist molecules induces some activation, and binding of three and four agonists progressively more activation<sup>8</sup>. Less is known about how ligand occupancy triggers desensitization, whether it involves cooperativity between the dimers<sup>23,24</sup>, and how different subunits contribute to

gating<sup>25-27</sup>. However, it has been proposed that binding of one ligand is sufficient to desensitize AMPA and kainate receptors<sup>22,28</sup>.

Channel opening and closing can be directly measured with high time resolution using patch clamp recordings. The means to control ligand binding, however, are limited. Fast ligand application can be achieved by fast solution switching or photo-uncaging<sup>29-31</sup>. However, at low ligand concentrations binding, a concentration-dependent step, becomes rate limiting and masks the gating process. Moreover, soluble ligands provide no control over which subunits get liganded. Indirect approaches to address multiple binding sites, such as the expression of mixtures or concatenated subunits with altered binding properties have proven difficult for studying iGluRs.

We established an alternative approach for manipulating ligand-controlled receptors with Photoswitched Tethered Ligands (PTLs), which were first developed on a nicotinic acetylcholine receptor<sup>32,33</sup> and later refined for the use as optogenetic tools<sup>34-39</sup>. Using a tethered glutamate agonist<sup>34,35</sup> and high light intensities, we achieved photoswitching and liganding on the sub-millisecond timescale, which made it possible to resolve the ligand-induced channel activation and desensitization of kainate receptors. This approach enabled us to probe the relation between ligand occupancy, activation and desensitization in homotetrameric GluK2 (iGluR6), as well as heteromeric GluK2/GluK5 (iGluR6/KA2) receptors. We obtained insight into how the binding of ligands drives desensitization and how it shapes the functional response in this major class of signaling molecules.

## Results

### Ligand binding in homotetrameric GluK2 receptors

The fast application of millimolar glutamate concentrations, mimicking synaptic release, results in sub-millisecond activation and opening of GluK2 channels, generating an inward current at negative membrane potentials (Fig. 1a). In the continued presence of glutamate, GluK2 desensitizes within milliseconds (Fig. 1a and Supplementary Results, Supplementary Fig. 1a,b). We were interested in how ligand binding at each of the subunits contributes to activation and desensitization. As described for GluK2<sup>16,27-29</sup>, lowering the glutamate concentration resulted in reduced activation, yet apparently full desensitization (Fig. 1a). However, the mechanistic interpretation of these dose-dependent experiments, is complicated for two general reasons: First, at low glutamate concentrations, the observed currents are dominated by the binding kinetics, rather than reflecting intrinsic receptor activation and desensitization. Second, low ligand concentrations lead to a low average occupancy of the four subunits, but will occasionally also lead to medium and high occupancy states (Fig. 1b and Supplementary Fig. 1c,d).

To circumvent these limitations, we made use of tethered photoswitchable MAG ligands (Fig. 1c,d)<sup>34,35</sup>. MAGs are based on an azobenzene switch that can be efficiently and reversibly photo-isomerized between a *trans* and *cis* configuration with light of specific wavelengths<sup>35</sup>. The ligand is covalently attached via its maleimide group to an engineered cysteine residue close to the binding site, e.g. L439C in GluK2 (Fig. 2a). The 4-alkylglutamate head-group serves as high efficacy agonist<sup>11</sup>, which in the *trans*

configuration points away from the binding site, while the *cis* form allows binding and activation.

We set out to utilize three key advantages of photoswitched tethered ligands: i) The azobenzene switch can be photo-isomerized in microseconds with light pulses that are tolerated by cells, providing a fast way to trigger ligand binding. ii) Ligand binding does not become rate limiting, but follows rapidly after switching into the *cis* configuration, because of the high effective concentration near the binding site ( $>10$  mM)<sup>35</sup>. This means even partially occupied states can be probed with high time resolution. iii) Ligand binding is restricted to labeled subunits with a cysteine attachment site, which allows targeting of specific subunits in heteromeric receptors.

### Fast photoswitching to resolve iGluR desensitization

Previous photoswitching experiments were performed at moderate light intensities<sup>32,33</sup> at which the observable activation kinetics reflected the progress of the photo-isomerization<sup>34,35</sup> (Supplementary Fig. 2), rather than *cis*-MAG binding and channel opening. To resolve the fast, physiologically relevant gating of kainate receptors we aimed for maximal photo-isomerization in considerably less than a millisecond. By combining 375 nm and 488 nm laser beams and focusing them in the sample plane of our recording setup, we obtained light intensities  $\sim 50$  W/mm<sup>2</sup> in a spot large enough to illuminate a cell or an excised membrane patch (Fig. 2b). At this irradiance, a 100  $\mu$ s light pulse of 375 nm light was more than sufficient to isomerize MAG into the activating *cis* configuration and to trigger maximal activation of GluK2 homotetramers expressed on the surface of HEK cells and labeled with MAG at position 439C (Fig. 2c,d). Channel activation was complete within a millisecond and was followed by rapid desensitization on the milliseconds timescale, resembling channel gating induced by brief glutamate applications (Fig. 1a). In an outside-out patch the current turned on with a rise time  $<50$   $\mu$ s ( $t_{10-90\%}$ , Supplementary Fig. 3a), indicating that isomerization and ligand binding occur on these or faster timescales. The lower time resolution of the whole-cell configuration underestimated the speed of opening (apparent rise times  $t_{10-90\%} \sim 50 - 200$   $\mu$ s), but was fast enough to accurately follow the slower process of desensitization ( $\tau = (3.7 \pm 0.8)$  ms, mean  $\pm$  s.d.,  $n = 24$  cells; Fig. 2e), similar to desensitization induced by glutamate (Supplementary Fig. 1a).

We found that a short 448 nm light pulse (100  $\mu$ s) was sufficient to induce full deactivation and led to channel closure in less than 1.5 ms (Supplementary Fig. 3b). This indicates that 488 nm light provides enough energy to *cis-trans* isomerize the bound MAG ligand and that unbinding of the low affinity *trans*-form is fast. When we applied the deactivation light pulse within a short interval after activation (2.5 ms) the receptors did not desensitize substantially (Supplementary Fig. 3c), as expected for brief ligand applications. These experiments show that photoswitching provides sub-millisecond control over ligand binding and unbinding and that *cis*-MAG acts as a potent agonist inducing fast activation and desensitization of GluK2 homotetramers.

Although MAG-induced desensitization was as fast, it was not as complete as induced by soluble glutamate. The substantial steady-state currents revealed varying degrees of desensitization across cells (Fig. 2f,  $n = 24$  cells and (Supplementary Fig. 4a). No further

desensitization occurred on long time scales (>10 s, Supplementary Fig. 4b). In contrast, glutamate caused almost full desensitization of GluK2 with steady-state currents <1 % (Supplementary Fig. 1a), and even low glutamate concentrations desensitize GluK2 homotetramers almost completely<sup>16,27-29</sup>. Similarly, glutamate desensitized our MAG-labeled GluK2 receptors and fully abolished the photo-responses (Supplementary Fig. 4c). Notably, the amount of photo-desensitization showed no correlation with the apparent time constant of desensitization (Supplementary Fig. 4d). Two general mechanisms could explain the substantial steady-state currents peculiar to photo-activation: i) Despite being activated, not all receptors might desensitize, perhaps because of incomplete labeling with MAG, or ii) recovery from the desensitized state might be so fast that a considerable fraction of the receptors will be activated at equilibrium.

To investigate the origin of the steady-state currents elicited by MAG photo-activation, we measured recovery from desensitization using repeated activation/deactivation cycles (Fig. 2g). After activating the receptors for 50 ms to achieve maximal desensitization we switched MAG to the *trans* form to induce ligand unbinding and to initiate recovery. After variable time delays (5 ms to 1 s), we used a second activation pulse to measure the fraction of receptors that had recovered in this interval. Recovery from MAG-induced desensitization ( $\tau = (155 \pm 31)$  ms, mean  $\pm$  s.d.,  $n = 10$ , Supplementary Fig. 4e-g) was considerably faster than recovery from glutamate-induced desensitization (Supplementary Fig. 1b), but still ~40 times slower than the apparent desensitization (Fig. 2e), and can therefore not explain the observed steady-state current. Moreover, the fraction of non-desensitizing current was constant in subsequent activations, but varied between cells. This behavior is consistent with variable MAG labeling that would result in differing amounts of two classes of photoswitched receptors: One receptor population that gets activated, desensitizes with a time constant of ~4 ms and recovers with a ~155 ms time constant, and a second population that gets activated, but never desensitizes. Consistent with this interpretation, the amount of desensitization did not correlate with the apparent kinetics of desensitization nor recovery (Supplementary Fig. 4d,g).

### Desensitization of partially occupied GluK2 homotetramers

To systematically test how high and low occupancy states control the desensitization of GluK2 receptors at a given level of labeling, we varied the intensity and/or duration of the 375 nm laser pulse to control the fraction of MAG ligands that is switched to the *cis* state. We triggered levels of activation that ranged from just above baseline (10 % of maximal current) up to full activation (Fig. 3a). As expected, the peak current saturated exponentially as we reached maximal, photo-stationary state levels of *cis*-MAG (Fig. 3b). Reduced photo-activation resulted in smaller currents, but the current rise and desensitization remained fast. The extent of desensitization, in contrast, changed with the degree of photoswitching (Supplementary Fig. 5a,b). With maximal activation, the receptors in the shown example desensitized to ~80 % (Fig. 3c), indicating a high level of MAG labeling (cf. Fig. 2f). At lower activation levels, the same receptor population desensitized considerable less and at the lowest intensities, desensitization was reduced to ~48 %, similar to the lower limit we observed across cells with what we interpret as variable MAG labeling (Fig. 2f). This confirmed that the degree of desensitization depends on the receptor occupancy, but not so

the apparent desensitization kinetics (Supplementary Fig. 5c,d). It is however difficult to relate specific desensitization behaviors to specific occupancies, since we probed receptor populations labeled to different amounts and in mixed patterns. For this, we turned to GluK2/GluK5 heteromers, which have defined 2:2 subunit stoichiometry and therefore allow to better control ligand occupancy.

### Subunit-specific activation of GluK2/GluK5 heteromers

Kainate receptors *in vivo* appear to be mostly heteromers of low affinity subunits like GluK2, and the high affinity subunits GluK4 and GluK5<sup>40-42</sup>. The assembly into GluK2/GluK5 heteromers affects receptor trafficking (Fig. 4a)<sup>43-46</sup>, as well as the functional properties<sup>27,28</sup>, but little is known about the mechanistic consequences of heteromer formation. GluK2/GluK5 heteromers emerge as particularly attractive model for biophysical studies, since they assemble with defined 2:2 stoichiometry<sup>46</sup>. Moreover, data on the isolated ATD assembly<sup>47</sup> suggests that the two subunit types might occupy particular positions within the tetramer. We used tethered MAG to selectively agonize the two GluK2 subunits with cysteines in position 439C and MAG labeling had no effect on wildtype GluK5 subunits (Supplementary Fig. 6a). We used 5-iodowillardiine (5-IW) to selectively activate the GluK5 subunits<sup>48</sup> (Supplementary Fig. 6b,c).

We co-expressed GluK2 and GluK5 subunits at a 1:3 transfection ratio to favor the formation of GluK2/GluK5 heteromers and to minimize the amount of GluK2 homomers (see Online Methods)<sup>27,28</sup>, while GluK5 subunits do not assemble into functional homotetramers<sup>40,44,45</sup>. To test, whether liganding of the two GluK2 subunits is sufficient to activate GluK2/GluK5 heteromers, we performed photoswitching experiments in the presence of concanavalin A (ConA) to suppress desensitization. Photo-stimulation of the MAG-labeled GluK2 subunits induced substantial currents of varying amplitude compared to activation by saturating glutamate concentrations (10 mM), the average being  $25 \pm 12$  % (mean  $\pm$  s.d.,  $n = 12$ ,  $max = 38$  %) (Fig. 4b). As we reasoned for GluK2 homotetramers, the observed range in activation efficiencies likely reflects different labeling efficiencies. Selective activation of the GluK5 subunits with saturating concentrations of 5-IW (1 mM) yielded  $40 \pm 11$  % (mean  $\pm$  s.d.,  $n = 10$  cells,  $max = 55$  %) of the glutamate-induced current (Fig. 4c). The maximal activation levels of 40 - 55 % achieved with either MAG or 5-IW are striking, given that only two out of four subunits are occupied (Supplementary Fig. 7). Simultaneous activation of the GluK2 and GluK5 subunits by MAG photoswitching and 5-IW application, respectively, evoked  $74 \pm 13$  % (mean  $\pm$  s.d.,  $n = 12$ ,  $max = 90$  %; Fig. 4d,e) of the glutamate-induced currents. This suggests that MAG and 5-IW in combination have an efficacy approaching that of glutamate (as shown earlier for MAG on GluK2 homotetramers<sup>35</sup>) and that the GluK2 and GluK5 subunits contribute roughly equal to receptor activation.

### Desensitization of partially occupied GluK2/GluK5 receptors

Having established that the GluK2 and GluK5 subunits, in conjunction with *cis*-MAG and 5-IW, yield efficient activation, we addressed their contributions to desensitization. In heteromeric receptors, slow photo-activation of GluK2 in the absence of ConA resulted in sizeable currents that were not significantly increased by the addition of ConA ( $0.93 \pm 0.20$



fold, mean  $\pm$  s.d.,  $n = 5$ ;  $p = 0.48$ , one sample  $t$ -test) (Fig. 5a), which suggests that ligand binding to the two GluK2 subunits does not induce substantial desensitization. On the other hand, slow photoswitching of GluK2 homotetramers resulted in strongly suppressed currents that were strongly increased by the addition of ConA ( $8.6 \pm 1.20$  fold, mean  $\pm$  s.d.,  $n = 4$  cells;  $p < 0.0011$ , one sample  $t$ -test) (Fig. 5a). This is expected since under these conditions desensitization was much faster than photoswitching ( $\tau_{\text{desen}} \sim 4$  ms, Fig. 2ef vs.  $\tau_{\text{photo on}} \sim 40$  ms, Supplementary Fig. 2).

To directly measure desensitization upon ligand binding to specific subunits, we turned to fast perfusion switching of soluble ligands and fast photoswitching of tethered ligands, respectively. We found, similar to earlier observations<sup>48</sup>, that GluK5 activation with 5-IW (1 mM) resulted in no or little desensitization of GluK2/GluK5 heterotetramers (Fig. 5b). 5-IW, however, induced full and prolonged desensitization of GluK2 homotetramers that carried a binding site substitution (N721S) to allow for 5-IW binding<sup>48</sup> (Fig. 5b; Supplementary Fig. 8a,b), like in GluK1 homotetramers that naturally respond to 5-IW<sup>48,49</sup>. Fast photo-liganding of the GluK2 subunits in cells expressing GluK2/K5 heterotetramers generated currents that rose as quickly as observed in GluK2 homotetramers, but which desensitized to only a minor amount ( $20.8 \pm 11.3$  %, mean  $\pm$  s.d.,  $n = 18$ ; Fig. 5c), significantly less than the lower limit of desensitization observed for partially labeled GluK2 homotetramers (Fig. 2f,  $\text{min} = 49.4$  %,  $p < 0.0001$ , one sample  $t$ -test). Likely, most or all of this desensitization can be attributed to a small fraction of GluK2 homotetramers that assembled alongside the GluK2/GluK5 heterotetramers<sup>28</sup>. Thus, while ligand binding to the two GluK2 subunits is sufficient to activate GluK2/GluK5 heteromers, it is apparently not sufficient to induce substantial desensitization.

Next we asked, what happens if both GluK2 and GluK5 are occupied with ligands. Photo-activation of the GluK2 subunits in the presence of saturating 5-IW concentrations had two consequences: the amplitude of the photo-current increased compared to only photo-liganding the GluK2 subunits (Fig. 5c and Supplementary Fig. 8c), and activation was followed by pronounced desensitization ( $102 \pm 10.4$  % of photo-current, mean  $\pm$  s.d.,  $n = 18$ , Fig. 5c, Supplementary Fig. 8d). In other words, co-activation of the GluK2 and GluK5 subunits induced strong desensitization, while activating them individually did not. As in GluK2 homotetramers the time constant of desensitization ( $\tau = (4.7 \pm 1.0)$  ms, mean  $\pm$  s.d.,  $n = 18$ , Supplementary Fig. S8e) did not depend on the ligand occupancy. Addition of glutamate fully desensitized the GluK2/GluK5 heteromers and suppressed any MAG-induced photo-current (Supplementary Fig. 8f).

We quantitatively analyzed this data on GluK2/GluK5 heteromers, taking partial MAG labeling into account (Supplementary Note 1). GluK2/GluK5 heteromers can have zero, one, or two labeled GluK2 subunits, but we assumed full occupancy of the two GluK5 subunits at saturating 5-IW concentrations. The photo-current relative to the 5-IW current then provides a measure of the labeling efficiency. With these assumptions we found that the total activation and potentiation of the photo-current was consistent with a model in which binding of one ligand gives no activation and an increase in subunit occupancy beyond one progressively increases activation (Supplementary Fig. 9a-c). A similar analysis for our desensitization data (Supplementary Fig. 9d-f) suggested that there was no desensitization



with one or two occupied subunits, but that ligand binding to a third subunit caused partial desensitization, and that full occupancy caused complete desensitization. Similarly, partial activation resulted in incomplete desensitization of GluK2 homotetramers. We summarized these results in a scheme depicting the different subunit types and occupancy states (Fig. 6a,b), however, we want to note that our ensemble measurements did not allow us to probe all states individually (Supplementary Fig. 10).

## Discussion

We employed a synthetic photoswitched tethered ligand to study how ligand binding to different subunits types drives activation and desensitization of a tetrameric signaling complex. Tethering of the ligand close to the binding site and the use of high light intensities enabled us to control binding and unbinding on the sub-millisecond timescale and to follow channel gating of homo- and heteromeric kainate receptors in real-time. The photo-activation resembled the activation by the natural agonist glutamate, validating the approach for biophysical studies and the optogenetic mimicry of synaptic signaling.

Photoswitched tethered ligands have been developed for a number of ion channels<sup>32-34,36,38,39</sup>, as well G protein-coupled receptors<sup>37</sup>. We found that biologically tolerated light intensities permit switching in tens of microseconds (the actual photo-isomerization of azobenzenes occurs within picoseconds). This is ideal for triggering conformational changes in neurotransmitter-gated receptors, similar to how voltage-steps can be used to probe voltage-gated ion channels. Ligand binding and unbinding can be reversibly induced or tested with high precision, and *on/off* light pulses can be combined to complex pulse protocols. The high effective ligand concentration in the liganding configuration allows to study ligand-induced conformational changes in systems, in which ligand binding is otherwise slow and rate-limiting.

Fast, ligand-induced desensitization is a hallmark of neurotransmitter-gated receptors. Here we asked, whether partial ligand binding induces desensitization of kainate receptors, namely in GluK2 homotetramers and the physiologically prevalent GluK2/GluK5 complex. Kinetic models based on studies with soluble ligands suggest that binding of only one ligand to the tetrameric receptors desensitizes them, but is not sufficient to activate them, *i.e.* that receptors get inactivated without channel opening (Supplementary Note 2 and Supplementary Fig. 11). The same models predict that desensitization gets faster as more ligands bind. Studies testing the regime of low ligand occupancies relevant to these predictions, however, were hampered by the slow on-rates at low ligand concentrations and the probabilistic binding to the four subunits.

Using tethered ligands, we found that the opposite is true and that limited binding of a high efficacy agonist activated kainate receptors without eliciting desensitization (Fig. 6). Multiple, and probably defined subunits have to be occupied to drive GluK2 homotetramers into the desensitized state. Consistent with this, liganding the GluK2 or GluK5 subunits in GluK2/GluK5 heterotetramers individually activated the receptors partially, but desensitization required ligand binding to both subunit types. Our findings do not conflict with earlier experiments, which showed that low glutamate concentrations lead to full

desensitization of GluK2 homotetramers without apparently opening them. The reason is that at low glutamate concentrations ( $\sim 10 \mu\text{M}$ ) activated channels never accumulate to substantial amounts, since binding is considerably slower than the subsequent desensitization<sup>29</sup>. Support for our findings also comes from the observation that very low glutamate concentrations ( $1 \mu\text{M}$ ) preferentially targeting the high affinity GluK5 subunits in GluK2/GluK5 heteromers yield substantial activation with no or very slow desensitization<sup>27</sup>, and from earlier demonstrations that GluK5-specific agonists cause activation without desensitization<sup>25,48</sup>.

What does this tell us about the molecular gating mechanism? iGluRs have four ligand binding sites and these are arranged in asymmetric complexes with subunits occupying inner and outer positions, as highlighted by the GluA2 homotetramer structure<sup>9</sup> (Fig. 6a). This arrangement might result in functional asymmetry and it has been proposed that the outer subunits couple more strongly to the gate<sup>9</sup>. The molecular architecture of GluK2/GluK5 heteromers is presently unknown, but we found that ligand binding to either the two GluK2, or GluK5 subunits opened the channel to similar extent (Fig. 6b). If the GluK2 and GluK5 subunits were to occupy defined positions as shown for the isolated GluK2/GluK5 amino-terminal domains<sup>47</sup>, this would argue against a strong functional difference between the inner and outer positions with respect to activation. However, we may have missed subtle differences due to incomplete labeling or different ligand efficacies, even though the MAG photoswitch and 5-IW together were similarly effective as glutamate.

A large body of structural and functional work suggests that rupture or rearrangement of the LBD dimer interfaces triggers desensitization<sup>13-20</sup>. However, how this rearrangement occurs in the context of the tetrameric receptors remains unclear<sup>22-27</sup>. We found that ligand binding to either the two GluK2 or the two GluK5 subunits did not induce desensitization, but that both subunit types had to be occupied to trigger desensitization (Fig. 6b). If the GluK2 and GluK5 subunits were to form LBD heterodimers (scenario A), this would indicate that the dimers operate as separate entities and that binding of one ligand does not provide enough energy to rearrange the dimer interface. If GluK2-GluK2 and GluK5-GluK5 LBD homodimers were to form (scenario B), this would mean that contributions from both dimers are necessary to desensitize the receptor. Recent work shows that GluK2 and GluK5 form ATD heterodimers<sup>47</sup>, which, with extrapolations from the GluA2 structure<sup>9</sup>, would result in a heterodimeric LBD arrangement (scenario A), although this awaits experimental verification. The fact that we observed partial desensitization with three bound ligands (Fig. 6b), lends some support to scenario A, suggesting that the LBD dimers operate as separate entities with respect to desensitization.

The dimeric LBD organization also appears to play an important role for desensitization in GluK2 homotetramers. We found that liganding of any single subunit did not cause desensitization, and at the limit of detectable activation, which is presumably reached with two occupied binding sites<sup>8</sup>, we only observed  $\sim 50\%$  desensitization (Fig. 3c). This indicates that some occupancy states with two ligands desensitized, while others did not, i.e. that desensitization depends on which specific subunits are occupied by agonist.

How might this affect iGluR signaling at synapses? The physiological function of iGluRs relies on detecting fast changes in glutamate concentration. Vesicular release from the nerve terminals leads to a rapid rise and fall of the glutamate concentration in the synaptic cleft: It is estimated to reach ~1 - 3 mM at the instant and site of release, but to drop to <0.3 mM by the time it diffuses 200 nm. Therefore many iGluRs will not be driven to full occupancy, before the glutamate concentration falls due to diffusion out of the synaptic cleft and reuptake. These considerations are particularly pertinent for kainate receptors with diverse pre- and postsynaptic functions<sup>3,4</sup> and occurrence at extra-synaptic locations, where glutamate has even more diverse concentration profiles. The partially liganded states we probed studying this study are hence likely to have important roles in shaping the dynamic range and kinetics of iGluRs, synaptic transmission and modulation.

We found that receptor desensitization is not directly coupled to activation, but that it depends on the ligand occupancy. We identified occupancy patterns that yield sustained activation without desensitization, a phenomenon that might be utilized by heteromeric iGluRs, such as GluK2/GluK5 heteromers incorporating high (GluK5) and low affinity (GluK2) subunits<sup>28,40,41</sup>. The high affinity subunits might be liganded by spilled-over glutamate from nearby synapses or glutamate released from astrocytes. Our model explains why low glutamate concentrations liganding the GluK5 subunits can elicit sustained activation until desensitization is triggered by an increase in glutamate that ligands the GluK2 subunits<sup>27</sup>. It also explains why subunit selective antagonists do not reduce the response to glutamate, but facilitate large non-desensitizing currents<sup>50</sup>. In homotetrameric receptors, activation and desensitization are more strongly linked, because glutamate binding occurs with similar affinity at all four subunits.

## Online Methods

### DNA constructs, expression in HEK cells, and MAG labeling

Rat GluK2a(Q) (K.M. Partin, Colorado State University) and GluK5 (P. Seeburg, MPI Heidelberg) were encoded on pcDNA or pRK expression plasmids. If not stated otherwise 'GluK2' denotes rat GluK2a(Q) including the L439C substitution for MAG labeling (this amino acid numbering includes the signal peptide). Site directed mutagenesis was confirmed by sequencing.

HEK 293T cells were grown in DMEM and 5 % FBS with 5 % CO<sub>2</sub> at 37 °C. For transfection, cells were plated on poly-lysine coated glass coverslips and transfected after 24 h using Lipofectamine 2000 (Invitrogen) with a total of ~0.3 - 0.5 µg DNA per ml medium. To identify transfected cells we co-transfected pNICE-YFP. Experiments were performed after 24 - 48 h expression for GluK2 homomers, and 48 - 72 h for GluK2/GluK5 heteromers, respectively. For co-expression of GluK2/GluK5 heteromers we used pRK GluK2 and GluK5 expression constructs at a 1:3 DNA ratio, respectively. Under these conditions we frequently observed a high amount of GluK2/GluK5 heteromers next to a minor fraction of GluK2 homotetramers, as described<sup>27,28</sup>. The high fraction of GluK2/GluK5 heteromers is further confirmed by the high amount of 5-IW currents compared to glutamate and the presence of their distinct desensitization behavior described in this study. Overall, the

expression of heteromers gave smaller currents<sup>28,45</sup>, probably due to reduced surface expression<sup>51</sup>.

All labeling experiments were performed using L-MAG-0 referred to as 'MAG' (**Fig. 1c** depicts the cysteine conjugate). The 4-alkylglutamic acid headgroup, resembling the high efficacy agonist (2*S*,4*R*)-4-methylglutamic acid (SYM 2081)<sup>11,52</sup>, serves as agonist. The synthesis of L-MAG-0 and the corresponding analytical data have been reported previously<sup>53</sup>. 50 mM stock solutions of L-MAG-0 were prepared in dry DMSO (Sigma, 99.9%, anhydrous). Before labeling, cells were washed with extracellular solution (see below), then MAG added to a final concentration of 40  $\mu$ M and incubated for 40 min at 37 °C in the dark. After labeling the cells were thoroughly rinsed with extracellular solution to remove any unreacted MAG.

### Patch clamp recordings, photoswitching and fast ligand application

Currents from HEK cells were recorded in the whole-cell or excised outside-out patch configuration at 22 - 24 °C using an Axopatch 200B headstage/amplifier, a Digidata 1440 A/D converter, and Clampfit Software (all Molecular Devices) on an inverted microscope (Olympus IX70). Standard chemicals were purchased from Sigma or Fisher Scientific. Recordings were performed in extracellular solution (138 mM NaCl, 1.5 mM KCl, 1.2 mM MgCl<sub>2</sub>, 2.5 mM CaCl<sub>2</sub>, 10 mM glucose, 10 mM HEPES, pH 7.3) with borosilicate glass patch pipettes. The pipettes had 3 - 7 M $\Omega$  resistance when filled with internal solution (122 mM CsCl, 2 mM NaCl, 2 mM MgCl<sub>2</sub>, 10 mM EGTA, 10 mM HEPES, pH 7.2). All experiments were performed in voltage clamp mode, typically at -75 mV. The pipette capacitance was compensated in cell-attached mode, and for fast whole-cell recordings series resistance was compensated. Data were filtered with the amplifier 4-pole Bessel filter at 1 kHz for slow perfusion experiments and 10 kHz for fast photoswitching, and typically recorded with 5 kHz or 50 kHz acquisition rates, respectively.

ConA, a lectin that has been shown to act with similar potency on GluK2 homomers and GluK2/GluK5 heteromers<sup>54</sup>, was used to irreversibly suppress desensitization. *Canavalia ensiformis* ConA was obtained from Sigma (L7647, type VI) and used without further purification at a concentration of 0.3 mg/ml in extracellular solution. It was either applied before and during MAG labeling (2 min pre-incubation time; **Fig. 4, Supplementary Figs. 2, 6 and 8a**), or added during the course of whole-cell recordings (**Fig. 5a**). In the latter case the maximal effect was typically achieved within 8 min after ConA addition.

L-Glutamate (Glu) was obtained from Sigma (49449, >99.5%), (S)-5-Iodowillardiine<sup>55</sup> (5-IW) from Tocris (0307, >98%). 5-IW is an agonist at GluK5 subunits (**Supplementary Fig. 6**) and on GluK2(N721S)<sup>48</sup>, where it has comparable efficacy to glutamate, whereas it does not activate and bind GluK2 receptors<sup>48,56</sup>. It had no agonistic or antagonistic effects on mutated GluK2(439C) subunits (**Supplementary Fig. 6a**).

Conventional photoswitching (**Fig. 4, Fig. 5a** and **Supplementary Figs. 2 and 6**) was performed using a DG4 Xe-lamp light source (Sutter, 300 W) coupled to the back port of an inverted IX70 microscope (Olympus) to give homogeneous epi-illumination through a 40x LUCPlanFLN NA 0.60 FN 22 UIS2 objective (Olympus). Band-pass filters (Semrock) were

used to select 379/34 nm and 500/24 nm light ('center'/'full width (>90% transmission)') light, which yielded light intensities (irradiance) of  $\sim 5$  mW/mm<sup>2</sup> and  $\sim 8$  mW/mm<sup>2</sup> in the sample plane, respectively. At these light levels the apparent time course of photo-activation is determined by the number of photons absorbed (**Supplementary Fig. 2**).

Fast, sub-millisecond photoswitching (**Fig. 2, Fig. 3, Fig. 5c** and **Supplementary Results**) was achieved with a laser spot illumination system, for which coupled the output of a 375/488 nm dual laser diode module (Omicron LDM: 375 nm 200 mW multi-mode, 488 nm 80 mW single-mode) into a UV/Vis multi-mode fiber (OZ Optics, 10  $\mu$ m, NA 0.1). The divergence of the exiting light was reduced by threefold magnification of the fiber end, collimated and directed to the back aperture of the objective (**Fig. 2b**). The light intensity (irradiance) in the sample plane was  $>50$  W/mm<sup>2</sup>. Pulsing of the laser diodes was controlled with TTL pulses, and the laser power with analog signals, both generated through the Clampex software and Digidata A/D converter (Molecular Devices). The timing and relative intensity of the laser pulses was measured above the sample stage using an amplified GaP photodiode PDA25K (Thorlabs).

Fast ligand application experiments (**Fig. 1, Fig. 5b** and **Supplementary Results**) were performed on outside-out patches with perfusion through a piezo-driven  $\theta$ -barrel<sup>57</sup>. The perfusion barrel was pulled from borosilicate glass (Warner Instruments, OD 2.0 mm, ID 1.40 mm, septum 0.2 mm) and broken with a diamond cutter to give a  $\sim 150$   $\mu$ m opening. The pipette was mounted on a piezo element (Physik Instrumente) and driven with voltage pulses from a MXPZT controller (Siskiyou). Flow of solutions (0.1 ml/min per barrel) was achieved with a syringe pump, in parallel to bath perfusion. Slow, whole bath perfusion of the diamond-shaped chamber (Warner Instruments, RC-25F) was performed with a gravity driven system at  $\sim 3$  ml/min.

### Data analysis and calculations

Data were analyzed with Clampfit (Molecular Devices) or Profit (Quantumsoft) and calculations performed with Matlab (Mathworks). Experiments were repeated several times after independent transfections. For fast photoswitching and ligand application experiments, 1 - 16 individual traces from a recording were averaged, and electrical artifacts removed for display. Where possible, data were averaged and reported with the standard deviations (s.d.) and the number of independent recordings (*n*). To test for statistical significance *Student's t-test* was used as indicated.

Throughout the main text we referred to receptor activation, desensitization and recovery as apparent processes observed as current rise phase, current decay and current reappearance in a test pulse after a preceding desensitization pulse, respectively. It should be noted that the given apparent rate constants are complex functions of all microscopic transitions present in the system. The use of kinetic models and microscopic rate constant is confined to **Supplementary Note 2**, incl. **Supplementary Fig. 11** and **Supplementary Table 1**.

The quantitative assessment of activation and desensitization in GluK2/GluK5 heteromers (**Supplementary Fig. 9**) is described in **Supplementary Note 1**. The equation used for fitting the data in **Supplementary Fig. 9a,d** was:

$y = f_1 \cdot a + f_2 \cdot b = (\sqrt{x} \cdot (1 - \sqrt{x}) \cdot 2) \cdot a + x \cdot b$ , where  $f_2 = x$ , and  $a$  and  $b$  are the relative contributions of single ( $f_1$ ) and double ( $f_2$ ) labeled receptors, respectively.

To evaluate the outcome of the linear kinetic models (see **Supplementary Note 2** and **Supplementary Fig. 11**) we used standard matrix methods<sup>58,59</sup>. For each model, all microscopic rate constants for the transitions between the accessible  $n$  states were listed in a  $n \times n$  rate constant matrix. First-order, or second-order rate constants multiplied with the respective ligand concentrations, were used as indicated (**Supplementary Fig. 11** and **Supplementary Table 1**). The apparent  $n - 1$  rate constants of the models were obtained as the eigenvalues of this matrix, and the corresponding amplitudes were obtained as spectral matrices calculated from the eigenvectors of this matrix and the condition that all receptors are in state R0 at time zero. For control purposes, we also calculated the population of the various states in small time steps by iteratively applying the corresponding differential equations, which gave identical results. All calculations were performed using standard Matlab procedures.

## Supplementary Material

Refer to Web version on PubMed Central for supplementary material.

## Acknowledgements

We thank Joshua Levitz for discussion, and we are grateful to Kathryn Partin and Peter Seeburg for the gift of clones, as well as to Dirk Trauner for the gift of L-MAG-0 and for many stimulating discussions. This work was supported by grants to E.Y.I. from the National Institutes of Health (2PN2EY018241 and U24NS057631) as well as a postdoctoral fellowship to A.R. from the Deutsche Forschungsgemeinschaft (DFG RE 3101/1-1).

## References

1. Dingledine R, Borges K, Bowie D, Traynelis SF. The glutamate receptor ion channels. *Pharmacol. Rev.* 1999; 51:7–61. [PubMed: 10049997]
2. Traynelis SF, et al. Glutamate receptor ion channels: structure, regulation, and function. *Pharmacol. Rev.* 2010; 62:405–496. [PubMed: 20716669]
3. Contractor A, Mulle C, Swanson GT. Kainate receptors coming of age: milestones of two decades of research. *Trend. Neurosci.* 2011; 34:154–163. [PubMed: 21256604]
4. Lerma J, Marques JM. Kainate receptors in health and disease. *Neuron.* 2013; 80:292–311. [PubMed: 24139035]
5. Mosbacher J, et al. A molecular determinant for submillisecond desensitization in glutamate receptors. *Science.* 1994; 266:1059–1062. [PubMed: 7973663]
6. Straub C, Tomita S. The regulation of glutamate receptor trafficking and function by TARPs and other transmembrane auxiliary subunits. *Curr. Opi. Neurobiol.* 2012; 22:488–495.
7. Christie LA, et al. AMPA receptor desensitization mutation results in severe developmental phenotypes and early postnatal lethality. *Proc. Natl. Acad. Sci. USA.* 2010; 107:9412–9417. [PubMed: 20439731]
8. Rosenmund C, Stern-Bach Y, Stevens CF. The tetrameric structure of a glutamate receptor channel. *Science.* 1998; 280:1596–1599. [PubMed: 9616121]
9. Sobolevsky AI, Rosconi MP, Gouaux E. X-ray structure, symmetry and mechanism of an AMPA-subtype glutamate receptor. *Nature.* 2009; 462:745–756. [PubMed: 19946266]
10. Jin R, Banke TG, Mayer ML, Traynelis SF, Gouaux E. Structural basis for partial agonist action at ionotropic glutamate receptors. *Nat. Neurosci.* 2003; 6:803–810. [PubMed: 12872125]



11. Mayer ML. Crystal structures of the GluR5 and GluR6 ligand binding cores: molecular mechanisms underlying kainate receptor selectivity. *Neuron*. 2005; 45:539–552. [PubMed: 15721240]
12. Stern-Bach Y, Russo S, Neuman M, Rosenmund C. A point mutation in the glutamate binding site blocks desensitization of AMPA receptors. *Neuron*. 1998; 21:907–918. [PubMed: 9808475]
13. Sun Y, et al. Mechanism of glutamate receptor desensitization. *Nature*. 2002; 417:245–253. [PubMed: 12015593]
14. Armstrong N, Jasti J, Beich-Frandsen M, Gouaux E. Measurement of conformational changes accompanying desensitization in an ionotropic glutamate receptor. *Cell*. 2006; 127:85–97. [PubMed: 17018279]
15. Weston MC, Schuck P, Ghosal A, Rosenmund C, Mayer ML. Conformational restriction blocks glutamate receptor desensitization. *Nat. Struc. Mol. Biol.* 2006; 13:1120–1127.
16. Paternain AV, Cohen A, Stern-Bach Y, Lerma J. A role for extracellular Na<sup>+</sup> in the channel gating of native and recombinant kainate receptors. *J. Neurosci.* 2003; 23:8641–8648. [PubMed: 14507963]
17. Plested AJ, Mayer ML. Structure and mechanism of kainate receptor modulation by anions. *Neuron*. 2007; 53:829–841. [PubMed: 17359918]
18. Chaudhry C, Weston MC, Schuck P, Rosenmund C, Mayer ML. Stability of ligand-binding domain dimer assembly controls kainate receptor desensitization. *EMBO J.* 2009; 28:1518–1530. [PubMed: 19339989]
19. Zhang Y, Nayeem N, Nanao MH, Green T. Interface interactions modulating desensitization of the kainate-selective ionotropic glutamate receptor subunit GluR6. *J. Neurosci.* 2006; 26:10033–10042. [PubMed: 17005866]
20. Dawe GB, et al. Defining the structural relationship between kainate-receptor deactivation and desensitization. *Nat. Struc. Mol. Biol.* 2013; 20:1054–1061.
21. Smith TC, Howe JR. Concentration-dependent substate behavior of native AMPA receptors. *Nat. Neurosci.* 2000; 3:992–997. [PubMed: 11017171]
22. Robert A, Howe JR. How AMPA receptor desensitization depends on receptor occupancy. *J. Neurosci.* 2003; 23:847–858. [PubMed: 12574413]
23. Robert A, Irizarry SN, Hughes TE, Howe JR. Subunit interactions and AMPA receptor desensitization. *J. Neurosci.* 2001; 21:5574–5586. [PubMed: 11466429]
24. Bowie D, Lange GD. Functional stoichiometry of glutamate receptor desensitization. *J. Neurosci.* 2002; 22:3392–3403. [PubMed: 11978816]
25. Swanson GT, et al. Differential activation of individual subunits in heteromeric kainate receptors. *Neuron*. 2002; 34:589–598. [PubMed: 12062042]
26. Mott DD, Rojas A, Fisher JL, Dingledine RJ, Benveniste M. Subunit-specific desensitization of heteromeric kainate receptors. *J. Physiol.* 2010; 588:683–700. [PubMed: 20026616]
27. Fisher JL, Mott DD. Distinct functional roles of subunits within the heteromeric kainate receptor. *J. Neurosci.* 2011; 31:17113–17122. [PubMed: 22114280]
28. Barberis A, Sachidhanandam S, Mulle C. GluR6/KA2 kainate receptors mediate slow-deactivating currents. *J. Neurosci.* 2008; 28:6402–6406. [PubMed: 18562611]
29. Heckmann M, Bufler J, Franke C, Dudel J. Kinetics of homomeric GluR6 glutamate receptor channels. *Biophys. J.* 1996; 71:1743–1750. [PubMed: 8889151]
30. Jayaraman V. Channel-opening mechanism of a kainate-activated glutamate receptor: kinetic investigations using a laser-pulse photolysis technique. *Biochem.* 1998; 37:16735–16740. [PubMed: 9843443]
31. Li G, Oswald RE, Niu L. Channel-opening kinetics of GluR6 kainate receptor. *Biochem.* 2003; 42:12367–12375. [PubMed: 14567698]
32. Bartels E, Wassermann NH, Erlanger BF. Photochromic activators of the acetylcholine receptor. *Proc. Natl. Acad. Sci. USA.* 1971; 68:1820–1823. [PubMed: 5288770]
33. Lester HA, Krouse ME, Nass MM, Wassermann NH, Erlanger BF. A covalently bound photoisomerizable agonist: comparison with reversibly bound agonists at Electrophorus electroplaques. *J. Gen. Physiol.* 1980; 75:207–232. [PubMed: 6246192]



34. Volgraf M, et al. Allosteric control of an ionotropic glutamate receptor with an optical switch. *Nat. Chem. Biol.* 2006; 2:47–52. [PubMed: 16408092]
35. Gorostiza P, et al. Mechanisms of photoswitch conjugation and light activation of an ionotropic glutamate receptor. *Proc. Natl. Acad. Sci. USA.* 2007; 104:10865–10870. [PubMed: 17578923]
36. Fehrentz T, Schönberger M, Trauner D. Optochemical genetics. *Angew. Chem.* 2011; 50:12156–12182. [PubMed: 22109984]
37. Levitz J, et al. Optical control of metabotropic glutamate receptors. *Nat. Neurosci.* 2013; 16:507–516. [PubMed: 23455609]
38. Tochitsky I, et al. Optochemical control of genetically engineered neuronal nicotinic acetylcholine receptors. *Nat. Chem.* 2012; 4:105–111. [PubMed: 22270644]
39. Kienzler MA, Reiner A, et al. A red-shifted, fast-relaxing azobenzene photoswitch for visible light control of an ionotropic glutamate receptor. *J. Am. Chem. Soc.* 2013; 135:17683–17686. [PubMed: 24171511]
40. Herb A, et al. The KA-2 subunit of excitatory amino acid receptors shows widespread expression in brain and forms ion channels with distantly related subunits. *Neuron.* 1992; 8:775–785. [PubMed: 1373632]
41. Wisden W, Seeburg PH. A complex mosaic of high-affinity kainate receptors in rat brain. *J. Neurosci.* 1993; 13:3582–3598. [PubMed: 8393486]
42. Contractor A, et al. Loss of kainate receptor-mediated heterosynaptic facilitation of mossy-fiber synapses in KA2<sup>-/-</sup> mice. *J. Neurosci.* 2003; 23:422–429. [PubMed: 12533602]
43. Gallyas F Jr, Ball SM, Molnar E. Assembly and cell surface expression of KA-2 subunit-containing kainate receptors. *J. Neurochem.* 2003; 86:1414–1427. [PubMed: 12950450]
44. Ren Z, et al. Multiple trafficking signals regulate kainate receptor KA2 subunit surface expression. *J. Neurosci.* 2003; 23:6608–6616. [PubMed: 12878702]
45. Nasu-Nishimura Y, et al. Identification of an endoplasmic reticulum-retention motif in an intracellular loop of the kainate receptor subunit KA2. *J. Neurosci.* 2006; 26:7014–7021. [PubMed: 16807331]
46. Reiner A, Arant RJ, Isacoff EY. Assembly stoichiometry of the GluK2/GluK5 kainate receptor complex. *Cell Rep.* 2012; 1:234–240. [PubMed: 22509486]
47. Kumar J, Schuck P, Mayer ML. Structure and assembly mechanism for heteromeric kainate receptors. *Neuron.* 2011; 71:319–331. [PubMed: 21791290]
48. Swanson GT, Green T, Heinemann SF. Kainate receptors exhibit differential sensitivities to (S)-5-iodowillardiine. *Mol. Pharm.* 1998; 53:942–949.
49. Cui C, Mayer ML. Heteromeric kainate receptors formed by the coassembly of GluR5, GluR6, and GluR7. *J. Neurosci.* 1999; 19:8281–8291. [PubMed: 10493729]
50. Pinheiro PS, et al. Selective block of postsynaptic kainate receptors reveals their function at hippocampal mossy fiber synapses. *Cer. Cortex.* 2012; 23:323–331.
51. Ma-Högemeier ZL, et al. Oligomerization in the endoplasmic reticulum and intracellular trafficking of kainate receptors are subunit-dependent but not editing-dependent. *J. Neurochem.* 2010; 113:1403–1415. [PubMed: 20050975]
52. Zhou LM, et al. (2S,4R)-4-methylglutamic acid (SYM 2081): a selective, high-affinity ligand for kainate receptors. *J. Pharm. Exp. Ther.* 1997; 280:422–427.
53. Numano R, et al. Nanosculpting reversed wavelength sensitivity into a photoswitchable iGluR. *Proc. Natl. Acad. Sci. USA.* 2009; 106:6814–6819. [PubMed: 19342491]
54. Everts I, Villmann C, Hollmann M. N-Glycosylation is not a prerequisite for glutamate receptor function but is essential for lectin modulation. *Mol. Pharm.* 1997; 52:861–873.
55. Patneau DK, Mayer ML, Jane DE, Watkins JC. Activation and desensitization of AMPA/kainate receptors by novel derivatives of willardiine. *J. Neurosci.* 1992; 12:595–606. [PubMed: 1371315]
56. Jane DE, et al. Synthesis of willardiine and 6-azawillardiine analogs: pharmacological characterization on cloned homomeric human AMPA and kainate receptor subtypes. *J. Med. Chem.* 1997; 40:3645–3650. [PubMed: 9357531]
57. Jonas, P. Fast application of agonists to isolated membrane patches.. In: Sakmann, B.; Neher, E., editors. *Single-Channel Recording*. Plenum Press; New York: 1995. p. 231-242.

58. Schwarz G. Kinetic analysis by chemical relaxation methods. *Rev. Mod. Phys.* 1968; 40:206–218.
59. Colquhoun, D.; Hawkes, AG. A Q-matrix cookbook.. In: Sakmann, B.; Neher, E., editors. *Single-Channel Recording*. Plenum Press; New York: 1995. p. 589-633.

Author Manuscript

Author Manuscript

Author Manuscript

Author Manuscript

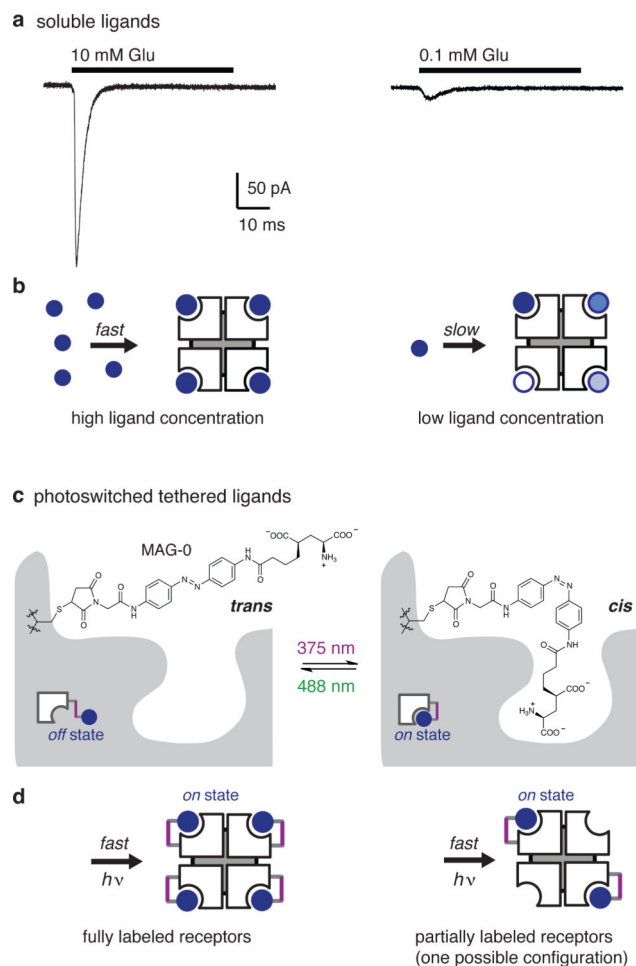


### Figure 1. Binding of soluble and tethered ligands

(a) Application of high, saturating glutamate concentrations leads to activation and subsequent desensitization of GluK2 homomers expressed in HEK cells. Lower glutamate concentrations give smaller, and apparently slower, but fully desensitizing currents. (b) Soluble ligands bind in a concentration-dependent manner (second-order process): High agonist concentrations result in fast binding and full receptor occupancy. Low ligand concentrations result in slow binding and give, on average, low receptor occupancies. However, high occupancy states are still populated, albeit with lower probabilities (indicated by lighter coloring, cf. **Supplementary Fig. 1c**). (c) Photoswitched tethered ligand: MAG-0 (maleimide-azobenzene-glutamate) is covalently attached to the ligand binding domain of GluK2 via coupling to an engineered cysteine residue (L439C). Azobenzene serves as photoswitch that can be rapidly isomerized between the *trans* and *cis* configuration with light of specific wavelengths. The headgroup, which is derived from the high efficacy agonist *S*4-methylglutamate, reaches the binding site only in the *cis* configuration<sup>34,35</sup>. (d) Tethered ligands associate in a fast, concentration independent manner (first-order process). The receptor occupancy is determined by the degree of labeling: Full labeling allows close to full occupancy, whereas partial labeling confines ligand binding to a specific subset of subunits.

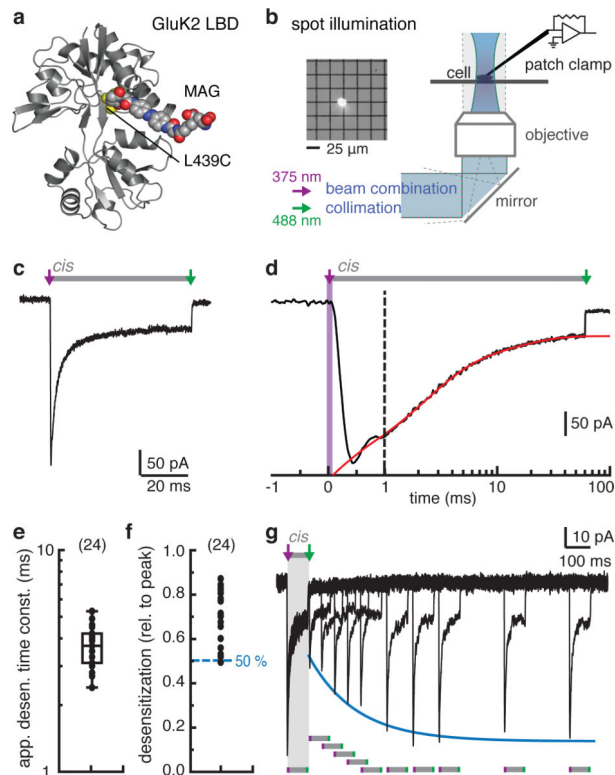


**Figure 2. Fast photoswitching of tethered agonists to probe activation and desensitization in GluK2 homotetramers with sub-millisecond precision**

(a) Structural model of MAG attached to the LBD of GluK2<sup>35</sup>. (b) Fast MAG photo-isomerization is achieved using a spot illumination system in combination with a patch-clamp setup. The inset shows a visualization of the high intensity light spot. (c-d) Activation and desensitization of GluK2 upon fast MAG photo-isomerization with a 100  $\mu$ s light pulse at 375 nm. Maximal channel opening is reached in less than a millisecond and is followed by fast desensitization. After 60 ms a 488 nm light pulse is applied to turn MAG back to the *trans* configuration. In this example the photo-current desensitizes with  $\tau = 3.4$  ms (red line) to 84 % of the peak current. (e) The apparent time constant of photo-induced desensitization is  $\tau = (3.7 \pm 0.8)$  ms (mean  $\pm$  s.d.,  $n = 24$  cells), similar to glutamate induced desensitization (**Supplementary Fig. 1a**). (f) The amount of desensitization ranges from 49 % to 87 % ( $n = 24$  cells). (g) Multi-pulse protocol to test recovery from desensitization: subsequent activation after different waiting times reveals that the steady-state current remains constant (see **Supplementary Fig. 4e-g**).

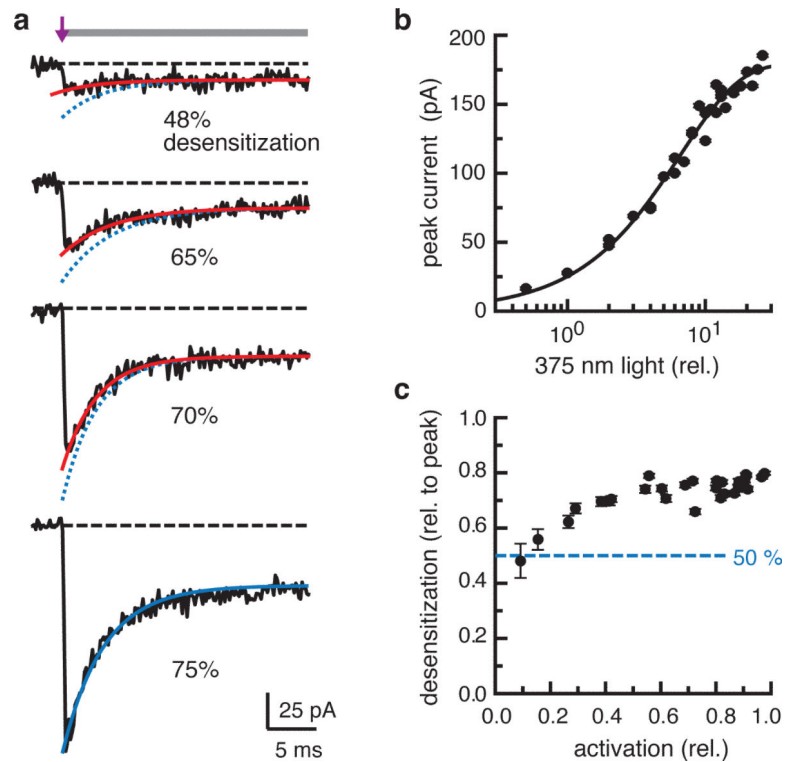


**Figure 3. The ligand occupancy determines the extent of desensitization in GluK2 homotetramers**

(a) Light stimuli of increasing power and duration are used to first partially, and then fully activate MAG-labeled GluK2 receptors (top to bottom). (b) The amount receptor activation (peak current) depends on the amount of photo-isomerization following an exponential relationship ( $k = 0.15 \text{ (V}\cdot\mu\text{s)}^{-1}$ ). (c) The relative amount of desensitization depends on the extent of activation, increasing from 48 % at the lowest stimulation levels to ~80 % (blue lines) at full stimulation. The error bars of the individual data points in panels **b** and **c** represent the confidence intervals as assessed by error analysis of the signal/noise ratio.

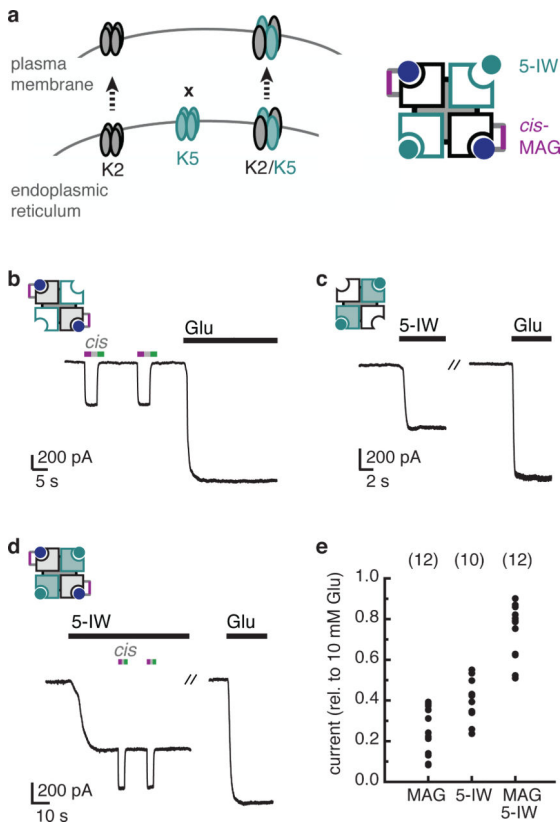


**Figure 4. Subunit-specific activation of GluK2/GluK5 heteromers with MAG and 5-IW**  
**(a)** GluK2 subunits assemble into homotetramers, whereas GluK5 subunits do not form functional receptors at the cell surface. Co-expression of GluK2 and GluK5 subunits yields heteromeric receptors with defined 2:2 subunit stoichiometry<sup>46</sup>. Photoswitchable ligands like MAG, which covalently attach to engineered cysteine residues, allow to restrict ligand binding to specific units, here to GluK2(439C) subunits. Conversely, the agonist 5-iodowillardiine (5-IW) can be used to specifically activate GluK5 over GluK2 subunits<sup>48</sup> (**Supplementary Fig. 6**). The cartoon does not intend to depict a specific subunit configuration, since it is not known, whether the GluK2 and GluK5 LBDs assemble as homodimers, heterodimers or in mixed configurations. **(b-e)** Subunit-specific activation GluK2/GluK5 heteromers in cells treated with ConA to suppress desensitization compared to activation of all four subunits with 10 mM glutamate. **(b)** Photo-activation of MAG labeled GluK2 subunits gives efficient activation of up to  $max = 38\%$  ( $n = 12$  cells) and **(c)** 5-IW (1 mM) mediated activation of GluK5 subunits up to  $max = 55\%$  activation ( $n = 10$  cells). **(d)** GluK2/K5 co-activation leads to activation to up to  $max = 90\%$  of saturating glutamate concentrations ( $n = 12$  cells). The variability observed for the activation levels achieved by photoswitching can be attributed to varying degrees of labeling.

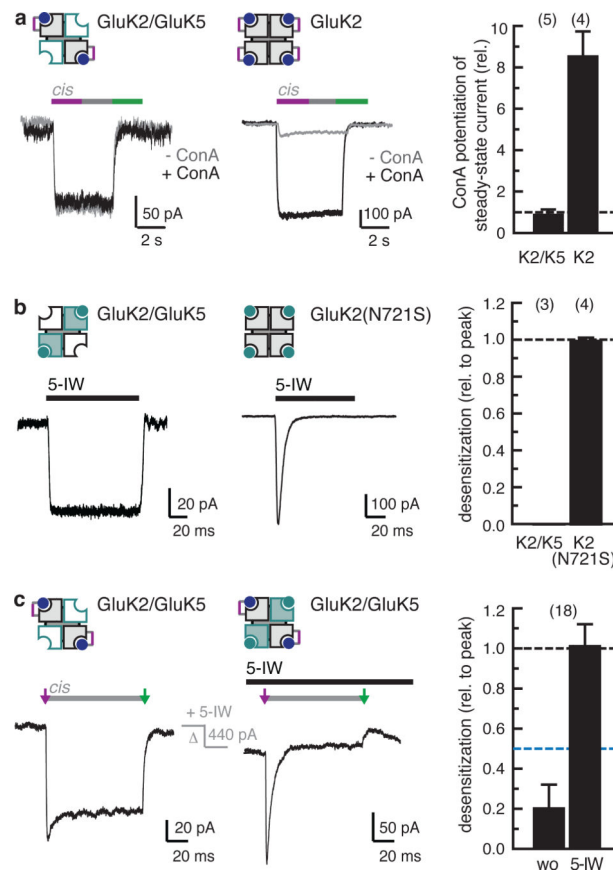


**Figure 5. Subunit-specific contributions to desensitization in GluK2/GluK5 heteromers**  
**(a)** Subunit-selective photoswitching of GluK2 subunits in cells expressing GluK2/GluK5 heteromers results in pronounced photo-currents that are not potentiated by the addition of ConA. Slow photoswitching of GluK2 homotetramers yields small steady-state currents that are strongly potentiated by ConA. **(b)** Fast application of 5-IW (1 mM), which only binds to the two GluK5 subunits, does not induce desensitization of GluK2/GluK5 heteromers. Fast application to GluK2 homotetramers carrying the N271S mutation that allows 5-IW binding at all four subunits, leads to full and fast receptor desensitization ( $\tau = (5.5 \pm 0.7)$  ms, mean  $\pm$  s.d.,  $n = 4$  patches). **(c)** Fast photoswitching of MAG-labeled GluK2 subunits in cells co-expressing GluK2 and GluK5. Photo-activation of just GluK2 subunits yields currents with no or little desensitization. The latter might point to the presence of a minor fraction of homomeric GluK2 receptors, which desensitize efficiently (see **Fig. 2f**). Addition of 5-IW to ligand the GluK5 subunits, photoswitching of the GluK2 subunits leads to fully desensitizing photo-currents. Panels on the right report means  $\pm$  s.d. with the number of experiments given in parentheses.



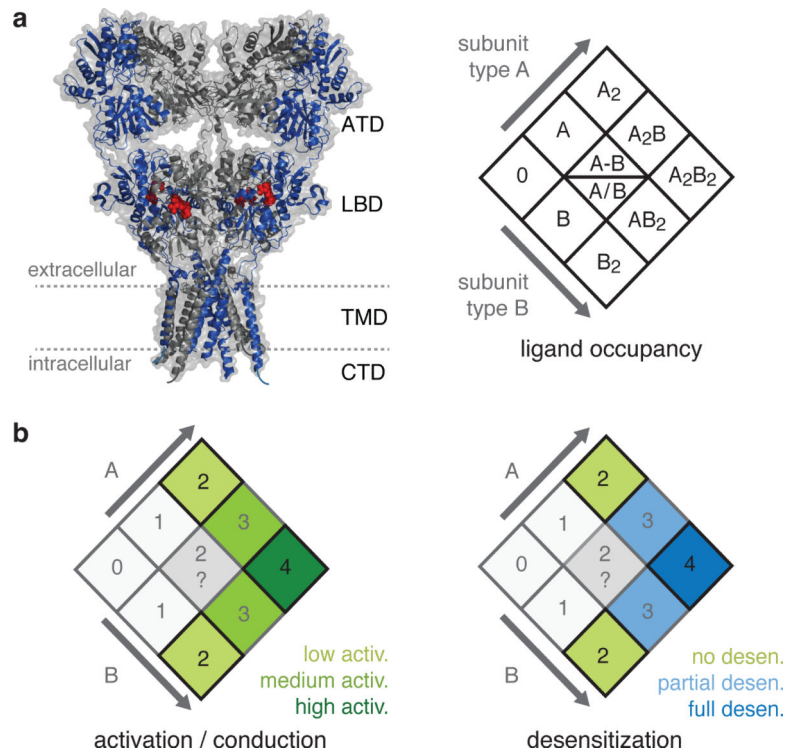


**Figure 6. Ligand occupancy, receptor activation and desensitization**

(a) iGluRs are asymmetric tetramers with two subunits occupying the inner positions (grey) and two subunits occupying the outer positions (blue)<sup>9</sup>. In heteromers these distinct positions might be taken by specific subunit types. The 2-fold symmetry gives rise to ten occupancy states. Four of these states can be attributed to binding of two ligands: Both ligands bound to the A subunits ( $A_2$ ), to the B subunits ( $B_2$ ), or mixed binding to the A and B subunits of the same dimer (A-B), or different dimers (A/B). (b) Left panel: Subunit-specific activation of GluK2/GluK5 heteromers showed that both subunit types give ~50 % activation, when two ligands are bound ( $A_2$  and  $B_2$ ). Previous data suggested that one ligand does not open kainate receptors efficiently, and, consistent with our data, that three ligands yield more activation than two, but less than four ligands. States unequivocally probed in this study are shown in black. We were not able to distinguish contributions from the A-B and A/B states. Right panel: Desensitization and ligand occupancy. We found no substantial desensitization of GluK2/GluK5 heteromers with only one subunit type occupied, that is no desensitization occurs from  $A_2$  and  $B_2$  states. Accordingly, partially labeled or partially activated GluK2 homomers desensitized partially, likely due to a mixture of  $A_2$ , A/B, A-B and  $B_2$  states. Our photoswitching experiments on GluK2/GluK5 heteromers further suggest that three occupied subunits give partial desensitization, whereas full occupancy ( $A_2B_2$ ) causes complete desensitization of homomers and heteromers.